

Predictive Modeling and Sensitivity Analysis for Averting Nanoparticle Agglomeration in Metal Matrices

Sanjay Gupta[#], Abhishek Tevatia^{#,*} and K.P.S. Rana[§]

[#]Department of Mechanical Engineering, Netaji Subhas University of Technology, Delhi - 110 078, India

[§]Department of Instrumentation and Control Engineering, Netaji Subhas University of Technology, Delhi - 110 078, India

*E-mail: abhishek.tevatia@nsut.ac.in

ABSTRACT

Nanoparticle agglomeration is a significant challenge in improving the properties of Metal Matrix Nanocomposites (MMNCs), as it leads to poor dispersion and weakens overall performance. Extensive experimental studies have explored ways to minimize agglomeration and identified key theoretical factors influencing this phenomenon. The present work formulates an effective yield strength prediction model that amalgamates several strengthening mechanisms - load transfer, increased dislocation density and Orowan strengthening. In addition, a degradation factor has also been included to address the effects of porosity. The model evaluates the impact of nanoparticle agglomeration on yield strength by introducing additional variables and identifies interfacial stress concentration and inadequate load distribution as primary contributors to strength reduction. It predicts a 69.29 % increase in yield strength with higher nanoparticle volume fractions, while larger nanoparticles (20-100 nm) and increased porosity (0-5 %) lead to reductions of 45.45 % and 5.50 %, respectively. Sensitivity analysis highlights key factors affecting yield strength, ensuring the model's robustness and practical relevance. Validated against established theoretical frameworks and empirical data, the model demonstrates high accuracy, instilling confidence in its predictions. This study presents a unified approach to quantifying the interplay between strengthening mechanisms and agglomeration effects, providing valuable insights for optimizing MMNCs in advanced engineering applications.

Keywords: Metal Matrix Nanocomposites (MMNCs); Yield strength; Strengthening mechanism; Nanoparticle agglomeration; Sensitivity analysis

NOMENCLATURE

$\Delta\sigma_{EDD}$: EDD enhancing yield strength strengthening (MPa)
$\Delta\sigma_{MSL}$: Strength due to load bearing effect (MPa)
$\Delta\sigma_{Orowan}$: Strengthening due to dislocation bowing (MPa)
$\Delta\sigma_{porosity}$: Deterioration factor with porosity (MPa)
C_b	: Volume of agglomeration
C_b^{np}	: Volume of nanoparticles in the agglomeration
C_m	: Volume the nanoparticle-free matrix
C_{np}	: Volume of the nanoparticle
C_u	: Volume of uniformly distributed nanoparticle region
C_u'	: Volume of nanoparticles in the uniformly distributed nanoparticle region
G_m	: Shear modulus of matrix (MPa)
V_m	: Volume fraction of matrix
V_{np}	: Volume fraction of nanoparticle
V_{np}^{agg}	: Volume fraction of nanoparticle agglomeration in the elementary volume
V_{np}^u	: Volume fraction of uniformly distributed nanoparticles in the elementary volume

V_p	: Volume fraction of porosity
d_{np}	: Particle size (nm)
f_{EDD}	: Improvement factor due to EDD
f_{MSL}	: Load bearing improvement factor
λ_b	: Volume fraction of nanoparticles in the agglomeration
ξ_b	: Volume fraction of agglomeration
ρ_{EDD}	: Enhanced density due to CTE mismatch (nm ⁻²)
$\sigma_{agg,nc}$: Overall influence of nanoparticle agglomeration in MMNCs, yield strength (MPa)
$\sigma_{b,ymc}$: Yield strength nanoparticle agglomeration region in the elementary volume (MPa)
$\sigma_{u,ymc}$: Yield strength nanoparticle uniformly distributed region in the elementary volume (MPa)
σ_{yc}	: Yield strength of composite material (MPa)
σ_{ym}	: Yield strength of the matrix material (MPa)
σ_{ymc}	: Yield strength by considering the effect of porosity (MPa)
σ_{ymc}	: Yield strength model considering the load bearing, dislocation density and Orowan strengthening mechanism (MPa)
\emptyset	: Empirical constant depends on the

	characteristics of porosity such as the size of pore, orientation, and geometry
ΔT	: Temperature change ($^{\circ}\text{C}$)
$\Delta\alpha$: CTE difference between the reinforcement phase and the matrix ($^{\circ}\text{C}^{-1}$)
C	: Elementary volume of MMNCs
a	: Aspect ratio
b	: Burger's vector of the matrix (nm)
k	: Constant
λ	: Inter-particles spacing (nm)

1. INTRODUCTION

Metal matrix composites (MMCs) are designed to enhance their physical and mechanical properties for load-bearing structural applications¹⁻³. However, there is a need for enhanced MMC materials in severe loads and environmental conditions^{2,4}. Nanotechnology advancements show that decreasing the size of reinforcing particles can enhance the properties of MMCs⁵⁻⁹. Metal Matrix Nanocomposites (MMNCs) are fabricated by dispersing reinforcing nanoparticles (≤ 100 nm) within a metal matrix, improving mechanical parameters like rigidity, yield strength, hardness, dimensional stability, malleability, and fatigue crack toughness^{5,10-13}. Strengthening mechanisms, such as the load transfer effect¹⁴, matrix Coefficient of Thermal Expansion (CTE)¹⁵, and Orowan strengthening¹⁶⁻¹⁸ plays a significant role in improving the overall strength of MMNCs. The soft matrix's strength is enhanced by transferring load to stronger reinforcement, resulting in a load transfer effect¹⁴. The distinct CTE between nanoparticles and metal matrix causes MMNCs to undergo dislocation during manufacturing, which can be strengthened by increasing the matrix dislocation density¹⁵. Orowan strengthening occurs due to nanoparticles hindering dislocation movement¹⁶⁻¹⁸.

Recent studies have focused on developing predictive models to determine the mechanical properties of MMNCs based on various metal matrices, reinforcement, and processing parameters^{16-17,19-23}. Ramakrishnan created a composite sphere model¹⁹ to estimate yield strength in micro-scaled discontinuous reinforced MMCs. Zhang and Chen¹⁶⁻¹⁷ improved Ramakrishnan's work by including Orowan strengthening, modulus mismatch, and load-bearing effects. Subsequent investigations have analysed the influence of dislocation density and thermal mismatch in enhancing these models^{16-17,23}, consequently broadening the comprehension of MMNC mechanical properties. However, porosity was not taken into consideration by the models, which might have resulted in exaggerated forecasts²⁴⁻²⁵.

Porosity can intermittently degrade reinforced MMNCs, creating stress concentration challenges and affecting properties like ductility and stiffness^{22,24-27}. According to Ahmad, *et al.*, porosity decreases strength and stiffness in cast discontinuous reinforced metal matrix composites²⁴. In addition, Ahmad²⁵, *et al.* William, *et al.* reported that porosity reduces ductility and fracture resistance. According to William, *et al.*, porosity acts as a stress concentrator, weakening carbon-carbon composites²⁶. Molina²⁷, *et al.* demonstrated that Al-Si/SiC composites with higher porosity have worse heat transfer efficiency. These findings demonstrate the importance of

porosity regulation during MMC production to improve mechanical integrity and thermal performance. The proportion of load-bearing reinforcing particles to vacant areas in MMNCs affects properties like ductility and stiffness. The presence of tiny holes from oxides and surrounded by reinforcing particles significantly diminishes the mechanical and thermal properties of MMNCs²⁸. Mirza and Chen²² developed a more accurate model for predicting yield strength by considering porosity.

Agglomeration of reinforced nanoparticles in MMNCs is another significant issue, restricting the improvement in mechanical and thermal properties²⁷⁻³¹. Exploring opportunities to predict nanoparticle agglomeration through computational modeling and simulation could minimize the effort, resources, and time required for extensive experimental investigations. The uniform distribution of nanoparticles in metal matrices is challenging due to properties like high viscosity and limited wettability in MMNCs²⁹⁻³⁰. Agglomeration, as shown in Fig. 1, is a phenomenon where loosely connected particles form compact clusters, and can be easily broken apart by physical forces^{29,31}. This can lead to composite failure at low stress. Agglomeration is caused by Van der Waals forces, electrostatic interactions, and high particle surface energy³¹. Research indicates that agglomeration in nanocomposites leads to high-stress regions and imperfections forming, causing a decline in mechanical parameters like elastic modulus, yield strength, and hardness of MMNCs²⁹⁻³⁵.

Pan and Bian²⁹ study various agglomeration variables that affect Carbon Nanotube (CNT) composite mechanical characteristics, emphasising the need for controlled dispersion, while Golbang³⁰, *et al.* have developed a quantitative approach to measure nanoparticle agglomeration. Pan and Bian³¹ study CNT composite thermal properties and how aggregation affects heat conduction channels. Qiao³², *et al.* studied how particle agglomeration and interphase growth affect the glass transition temperature of nanocomposites, revealing complex nanoscale interactions. Zare³³ models nanocomposites' yield strength using nanoparticle agglomeration and interphase effects. Shi³⁴, *et al.* demonstrate that non-uniform CNT waviness and agglomeration reduce reinforced composite rigidity. Interphase modulus and nanofiller agglomeration in polypropylene nanocomposites affect tensile modulus, according to Karevan³⁵, *et al.* These studies underline the importance of nanoparticle dispersion in composite quality and the need for advanced agglomeration control for enhanced mechanical and thermal performance. Therefore, identifying and assessing the aggregation status of nanoparticles is crucial.

Existing models cannot accurately account for the effects of nanoparticle agglomeration and porosity, despite significant advancements in integrating multiple strengthening mechanisms. By integrating load transfer, enhanced dislocation density, Orowan strengthening, and porosity quantification, this study enhances the prediction of yield strength in MMNCs, thereby addressing this lacuna. The current approach offers a comprehensive and precise evaluation of mechanical behaviour, in contrast to previous models that examined these mechanisms in isolation. Additionally, a novel sensitivity analysis is introduced to systematically assess the impact of fundamental parameters, thereby improving the practical applicability and

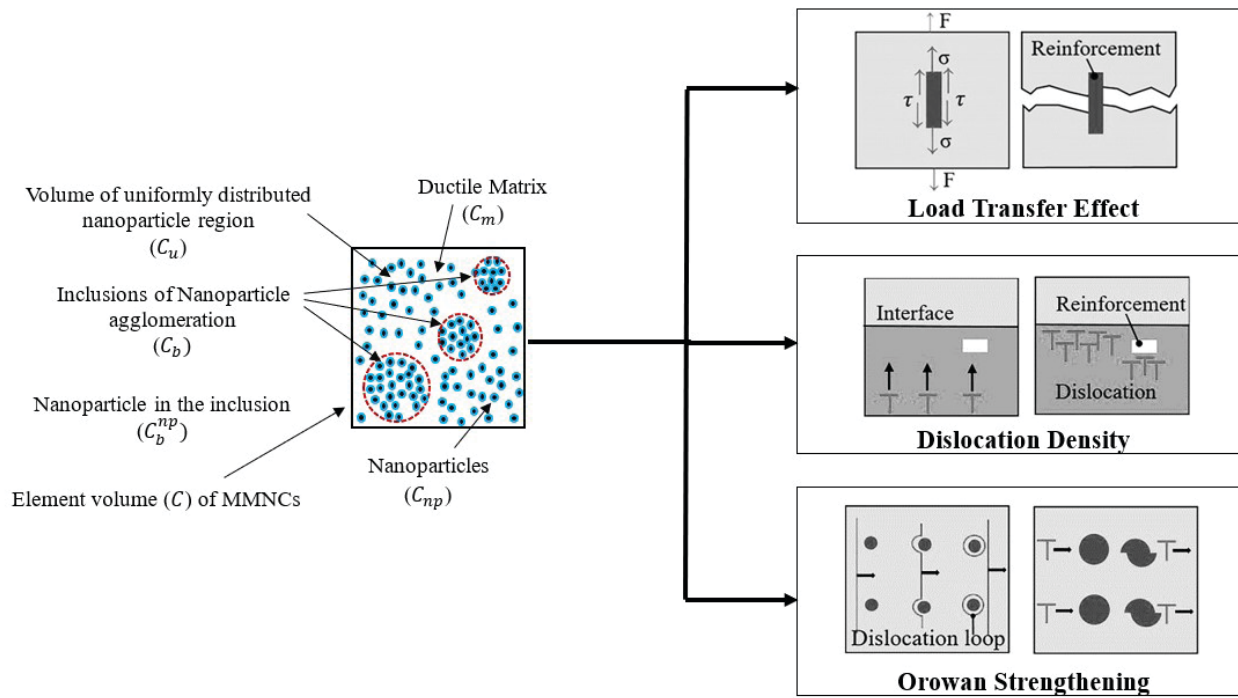


Figure 1. Illustration of the element volume of MMNCs with uniformly and non-uniformly distributed (agglomerated) nanoparticles and a schematic of the MMNCs strengthening mechanism.

robustness of the model. This study optimises the properties of MMNC and guarantees the reliability of predictions by evaluating parameter variability. By incorporating multiple strengthening mechanisms into a single predictive model, the proposed framework represents a substantial advancement, providing valuable insights for computational modelling and experimental validation.

2. NANOPARTICLE AGGLOMERATION

The dispersion of nanoparticles throughout the metal matrix significantly affects the effective properties of MMNCs. However, in a few cases, due to the fabrication process of MMNCs, nanoparticle agglomeration has been reported³⁶⁻³⁷. It is vital to account for nanoparticle agglomeration in the analysis of nanoparticle reinforced MMNCs. Figure 1 shows the nanocomposite's elementary volume as C , which has two regions: the volume of the nanoparticle (C_{np}) and the volume of the nanoparticle-free matrix (C_m)

$$C_{np} + C_m = C \quad (1)$$

The average volume fraction of nanoparticles can be represented as follows.

$$V_{np} = \frac{C_{np}}{C} \quad (2)$$

The volume fraction of matrix is V_m is evaluated as follows.

$$V_m = 1 - V_{np} \quad (3)$$

where, V_{np} is the volume fraction of nanoparticle. If C contains agglomeration as depicted in Fig. 1, then the volume of agglomeration is C_b and further, the volume of uniformly distributed nanoparticle region C_u is calculated as follows.

$$C_u = C - C_b \quad (4)$$

The volume of nanoparticles in the agglomeration is C_b^{np} and the volume of nanoparticles in the uniformly distributed nanoparticle region $C_u^{np} = C - C_b^{np}$. The micromechanical agglomeration model has been formulated by introducing two agglomeration parameters.

$$\xi_b = \frac{C_b}{C} \quad \& \quad \lambda_b = \frac{C_b^{np}}{C_{np}} \quad (5)$$

where, ξ_b is the volume fraction of agglomeration, and λ_b is the volume fraction of nanoparticle in the agglomeration. Using Eqn. (2 & 5), in regions with high nanoparticle concentrations, the volume fraction of nanoparticle agglomeration/ inclusion V_{np}^{agg} is given by,

$$V_{np}^{agg} = \frac{C_b^{np}}{C_b} = \frac{\lambda_b}{\xi_b} V_{np} \quad (6)$$

The nanoparticle volume fraction is computed for the region with uniformly distributed nanoparticles.

$$V_{np}^u = \frac{C_u^{np}}{C_u} = \frac{(C_{np} - C_b^{np})}{C - C_b} = \frac{(1 - \lambda_b)}{(1 - \xi_b)} V_{np} \quad (7)$$

3. STRENGTHENING MECHANISM

Nanoscale reinforcements, typically less than 100 nm, enhance the mechanical properties of MMNCs⁵. These reinforcements, including nanoparticles, nanofibers, and nanowires, enhance the metal matrix's strength, hardness, and other mechanical properties. The selection of nanoparticles, their size, distribution, volume percentage, and processing methods significantly impact the effectiveness of strengthening processes in MMNCs^{5,10-11}. Researchers and engineers can optimize these parameters for specific applications. The common strengthening mechanisms^{16-17,19-22} of MMNCs are considered as follows.

3.1 Load Transfer to the Reinforcement Particles

Load bearing refers to the transfer of shear loads from a soft metal matrix to discontinuous reinforced nanoscale particles in MMNCs^{14,23}. The effectiveness of a mechanism depends on the successful cohesion between the matrix and reinforcement materials. The shear lag model is used when there is significant cohesion between reinforced particles and the metal matrix. This is achieved by leveraging nano-sized reinforcement particles and effective fabrication techniques. The ability of nano-sized particles to bear specific loads is influenced by volume fraction and load transfer between the matrix and reinforcement. Hard non-shearable nanoparticles in nanocomposites enhance stiffness through interfacial shear load transfer^{14,16-17}. A shear lag model was proposed^{16,23} as represented in Eqn. (8).

$$\sigma_{yc} = \sigma_{ym} \left[\frac{V_{np}(a+2)}{2} + V_m \right] \quad (8)$$

where, a is the aspect ratio (generally $a \cong 1$ for equiaxed components). Considering $V_{np} + V_m = 1$ then Eqn. (8) may be rewritten as Eqn. (9).

$$\sigma_{yc} = \sigma_{ym} \left[\frac{V_{np}}{2} + 1 \right] \quad (9)$$

The strengthening due to the MSL model mechanism in the absence of porosity is evaluated as follows.

$$\Delta \sigma_{MSL} = \frac{1}{2} V_{np} V_m \quad (9a)$$

The porosity present in MMNCs materials does affect the load-bearing reinforcement mechanism. The effect of the volume fraction of porosity V_p is considered as $V_{np} + V_m + V_p = 1$, into Eqn. (8), and then the strengthening due to this mechanism of MMNCs in the presence of porosity²² is given by Eqn. (9b).

$$\Delta \sigma_{MSL} = \sigma_{ym} \left(\frac{1}{2} V_{np} - V_p \right) \quad (9b)$$

Finally, the improvement factor due to this mechanism can be expressed as follows.

$$f_{MSL} = \frac{\Delta \sigma_{MSL}}{\sigma_{ym}} \quad (10)$$

3.2 Dislocation Density

Researchers have found that the mechanical properties of MMNCs are significantly improved due to the increased interfacial area between reinforcement nanoparticles and the matrix. This interfacial area is crucial for overall performance enhancement^{16-17,19}. Thermal mismatch dislocations are generated in the matrix surrounding nano-sized particles to alleviate thermal stresses from the cooling process^{5,14-15,38}. Thermal stresses near nanoparticles change significantly, leading to plastic deformation within the matrix. Thermal misfit strains alter the internal stress state at the interface between the matrix and particles^{14-15,38}. The phenomenon of prismatic punching of dislocations at the interface reduces stored energy, while strain hardening near the interface increases the matrix's strength^{5,15,38}. If the span of a produced dislocation loop is πd_p , at that moment, the EDD enhancing yield strength strengthening $\Delta \sigma_{EDD}$ can be evaluated^{16-17,19} by Eqn. (11).

$$\Delta \sigma_{EDD} = k G_m b \sqrt{\rho_{EDD}} \quad (11)$$

$$\rho_{EDD} = \frac{12 \Delta \alpha V_{np} \Delta T}{(1 - V_{np}) b d_{np}} \quad (12)$$

Finally, the improvement factor due to the CTE mismatch mechanism is expressed as follows:

$$f_{EDD} = \frac{\Delta \sigma_{EDD}}{\sigma_{ym}} \quad (13)$$

where, G_m is shear modulus of the matrix, b is burger's vector of the matrix, k is a constant ($k \approx 1.25$), based on theoretical estimates¹⁶, ρ_{EDD} is enhanced density due to CTE mismatch, d_{np} is particle size, $\Delta T = T_{process} - T_{test}$ is temperature change, $\Delta \alpha = \alpha_m - \alpha_p$ is the CTE difference between the reinforcement phase and the matrix.

3.3 Orowan Strengthening

Orowan strengthening effects are observed in discontinuously reinforced MMNCs, where rigid particles impede dislocation motion¹⁸. However, the significance of Orowan strengthening in microsized particulate-reinforced metal MMCs is limited due to the coarse size of reinforcement particles and large interparticle spacing. The presence of reinforcement particles is often localized along the grain boundaries of the matrix material, raising questions about its feasibility^{5,16-17}. Orowan strengthening in melt-processed MMCs is not a significant factor, but rather due to highly dispersed nanosized reinforcement particles (≤ 100 nm) within the metal matrix. These particles act as obstructions, causing dislocation lines to bend initially but eventually reconnect and form a loop. Certain activities can generate counteracting stress, posing challenges for dislocation movement and increasing yield stress. Higher stress is necessary for enhanced composite material strength^{5,16-17}. The strengthening $\Delta \sigma_{Orowan}$ due to this strengthening mechanism of dislocation bowing is evaluated³⁹ by Eqn. (14).

$$\Delta \sigma_{Orowan} = \frac{0.13 G_m b}{\lambda} \ln \left(\frac{d_{np}}{2b} \right) \quad (14)$$

$$\lambda = d_{np} \left[\left(\frac{1}{2V_{np}} \right)^{\frac{1}{3}} - 1 \right] \quad (15)$$

Finally, the improvement factor is obtained as follows.

$$f_{Orowan} = \frac{\Delta \sigma_{Orowan}}{\sigma_{ym}} \quad (16)$$

where, λ =inter-particles spacing (nm), b =burgers vector (nm) & G_m =shear modulus (GPa).

3.4 Porosity

Porosity in MMNCs significantly impacts their load-bearing capacity and yield strength. This porosity leads to stress concentration, crack initiation, and propagation, affecting the composite's mechanical properties^{22,24-27}. Discontinuities in high-stress components initiate fatigue cracks^{12-13,40}. The current study examined the impact of increasing reinforcement particle volume fraction on void formation and yield strength. Results prove that as reinforcement particle volume fraction increased, the probability of void formation also increased, leading to a noticeable degradation of yield strength^{22,25,27}.

To accurately predict the yield strength of MMNCs, it is imperative to consider the influence of porosity²² as follows.

$$\Delta \sigma_{porosity} = \sigma_{ym} (1 - e^{-\emptyset V_p}) \quad (17)$$

The deterioration factor²⁶ with porosity in MMNCs is expressed by Eqn. (17a).

$$f_{porosity} = 1 - e^{-\emptyset V_p} \quad (17a)$$

where, \emptyset is the empirical constant and depends on the characteristics of porosity, such as the size of the pore, orientation, and geometry²⁶. If the shape of the pore is cylindrical with orientation between 40°-90° to the loading axis, the value of \emptyset is computed as $\emptyset = 0.405 l_{np} / d_{np} + 0.318 d_{np} / l_{np} + 1.22^{26}$, l_{np} is the length of the nanoparticle and in the present case, the particle shape is cubic, i.e., $\emptyset = 1.943$.

4. YIELD STRENGTH MODEL: NANOPARTICLE AGGLOMERATION

The yield strength model assumes homogeneous dispersion of nanoparticles, excepting agglomerated regions, and adopts ideal spherical or cubic nanoparticle geometries for simplicity. The effects of interfacial bonding, strain rate variations, and temperature fluctuations are not considered, potentially resulting in discrepancies from actual material behaviour. The yield strength model considering the load bearing, dislocation density and Orowan strengthening mechanism can be derived considering strengthening improvement factors (Eqn. 10, Eqn. 13 & Eqn. 16) using the compounding summation technique^{16-17,19} as follows.

$$\sigma'_{ync} = \sigma_{ym} (1 + f_{MSL}) (1 + f_{EDD}) (1 + f_{orowan}) \quad (18)$$

Eqn. 18 formulates an effective yield strength prediction model amalgamating several strengthening mechanisms: load transfer, increased dislocation density, and Orowan strengthening.

The proposed model to predict the yield strength by considering the effect of porosity in the MMNCs is evaluated as in Eqn. (19).

$$\sigma_{ync} = \sigma'_{ync} (1 - f_{porosity}) \quad (19)$$

Substituting the values of all improvement factors in Eqn. (19) as:

$$\sigma_{ync} = \sigma_{ym} \left\{ \left(1 + \frac{1}{2} V_{np} - V_p \right) \left(1 + \frac{3.464kG_m}{\sigma_{my}} \sqrt{\frac{b \Delta \alpha \Delta TV_{np}}{d_{np} (1 - V_{np})}} \right) \left(1 + \frac{0.13G_m b}{d_{np} \left[\left(\frac{1}{2V_{np}} \right)^{\frac{1}{3}} - 1 \right] \sigma_{my}} \ln \left(\frac{d_{np}}{2b} \right) \right) \left(1 - (1 - e^{-\emptyset V_p}) \right) \right\} \quad (20)$$

To accurately assess the yield strength of MMNCs, it is necessary to consider the occurrence of nanoparticle agglomeration. This is achieved by including both the uniform and agglomerated regions in the investigation as depicted in Fig. 1. The yield strength ($\sigma_{b,ync}$) of the region with nanoparticle agglomeration in the elementary volume (C) of MMNC is evaluated by replacing (V_{np}) with (V_{np}^{agg}) in Eqn. (20).

$$\sigma_{b,ync} = \sigma_{ym} \left\{ \left(1 + \frac{1}{2} V_{np}^{agg} - V_p \right) \left(1 + \frac{3.464kG_m}{\sigma_{my}} \sqrt{\frac{b \Delta \alpha \Delta TV_{np}^{agg}}{d_{np} (1 - V_{np}^{agg})}} \right) \left(1 + \frac{0.13G_m b}{d_{np} \left[\left(\frac{1}{2V_{np}^{agg}} \right)^{\frac{1}{3}} - 1 \right] \sigma_{my}} \ln \left(\frac{d_{np}}{2b} \right) \right) \left(1 - (1 - e^{-\emptyset V_p}) \right) \right\}$$

$$\left\{ \left(1 + \frac{0.13G_m b}{d_{np} \left[\left(\frac{1}{2V_{np}^{agg}} \right)^{\frac{1}{3}} - 1 \right] \sigma_{my}} \ln \left(\frac{d_{np}}{2b} \right) \right) \left(1 - (1 - e^{-\emptyset V_p}) \right) \right\} \quad (21)$$

The yield strength ($\sigma_{u,ync}$) of the region with uniformly distributed nanoparticles in the elementary volume (C) of MMNC may be evaluated by replacing V_{np} with V_{np}^u in Eqn (20).

$$\sigma_{u,ync} = \sigma_{ym} \left\{ \left(1 + \frac{1}{2} V_{np}^u - V_p \right) \left(1 + \frac{3.464kG_m}{\sigma_{my}} \sqrt{\frac{b \Delta \alpha \Delta TV_{np}^u}{d_{np} (1 - V_{np}^u)}} \right) \left(1 + \frac{0.13G_m b}{d_{np} \left[\left(\frac{1}{2V_{np}^u} \right)^{\frac{1}{3}} - 1 \right] \sigma_{my}} \ln \left(\frac{d_{np}}{2b} \right) \right) \left(1 - (1 - e^{-\emptyset V_p}) \right) \right\} \quad (22)$$

The yield strength is evaluated using Eqn. (21 & 22) to account for the overall influence of nanoparticle agglomeration in MMNCs.

$$\sigma_{agg, nc} = \xi_b \sigma_{b,ync} + (1 - \xi_b) \sigma_{u,ync} \quad (23)$$

The above model predicts the yield strength of MMNCs for various combinations of metal matrix and nanoparticles, while considering the phenomenon of nanoparticle agglomeration.

5. RESULTS AND DISCUSSION

The current study intends to gain insights into the mechanical behavior of MMNCs, especially yield strength, by analyzing the effect of porosity and nanoparticle agglomeration. Table 1 presents a comprehensive summary of the mechanical properties and different modeling parameters used in this investigation. The proposed model is being compared with other available models^{16-17,19-23} and validated by experimental data⁶⁻⁸ of MMNC materials. Further, the combined effect of strengthening mechanisms, porosity, and agglomeration on MMNC yield strength is examined. The comprehensive study has analyzed the predictive model's sensitivity to determine how the input factors affect the output parameter, MMNC yield strength.

5.1 Effectiveness of the Yield Strength Model

The study compares seven different models for Al_2O_3 nanoparticle reinforced in Mg matrix and validated by experimental data^{16,19-23} as shown in Fig. 2(a). The results show that the predicted yield strength is comparable to the experimental value when the nanoparticle volume fraction is 1.1 %. Out of the seven models, four models underestimate the yield strength, while the three models, including the Ramakrishnan Model¹⁹, Zhang & Chen Model¹⁶, and the present model, predicted the yield strength with accuracy close to experimental data. The underestimated results can be attributed to the absence of the combined effect of different strengthening mechanisms in these models. Only the present model considers the effect of porosity and nanoparticle agglomeration.

The existing model results in variable predictions, possibly due to surface flaws and heterogeneity^{22,25,28}. Microstructural heterogeneity may result in low yield strength, specifically, pores and agglomeration in MMNCs. High-stress concentrations at pore tips and lower deformation of MMNCs accelerate void coalescence and fracture propagation^{12,28}. The

Table 1. Mechanical properties and modelling parameters for MMNCs considered

Parameter	Mg-Al ₂ O ₃	Mg-SiC	Mg-Y ₂ O ₃	Mg-ZrO ₂	Mg-CNT	Al-SiC	Al-Al ₂ O ₃	Al7075-TiB ₂	Ti-Y ₂ O ₃
V_p (%)	1	1	1	1	1	1	1	1	1
k	1.25	1.25	1.25	1.25	1.25	1.25	1.25	1.25	1.25
G_m (GPa)	16.5	16.5	16.5	16.5	16.5	25.9	25.9	71.7	44.8
b (nm)	0.32	0.32	0.32	0.32	0.32	0.286	0.286	0.286	0.29
$\Delta\alpha$ (°C ⁻¹) $\times 10^{-6}$	21	24	19	18	30	18.3	16	18.3	2.6
ΔT (°C)	280	280	280	280	330	475	500	475	880
d_{np} (nm)	50	50	50	50	30	50	50	50	40
\emptyset	1.943	1.943	1.943	1.943	1.943	1.943	1.943	1.943	1.943
σ_{ym} (MPa)	97	97	97	97	97	100	83	455	450
References	5-8,26	5,22,26	5,16,26	5,26,41	5,26,41	5,12	5,12	5,28	5,16,41

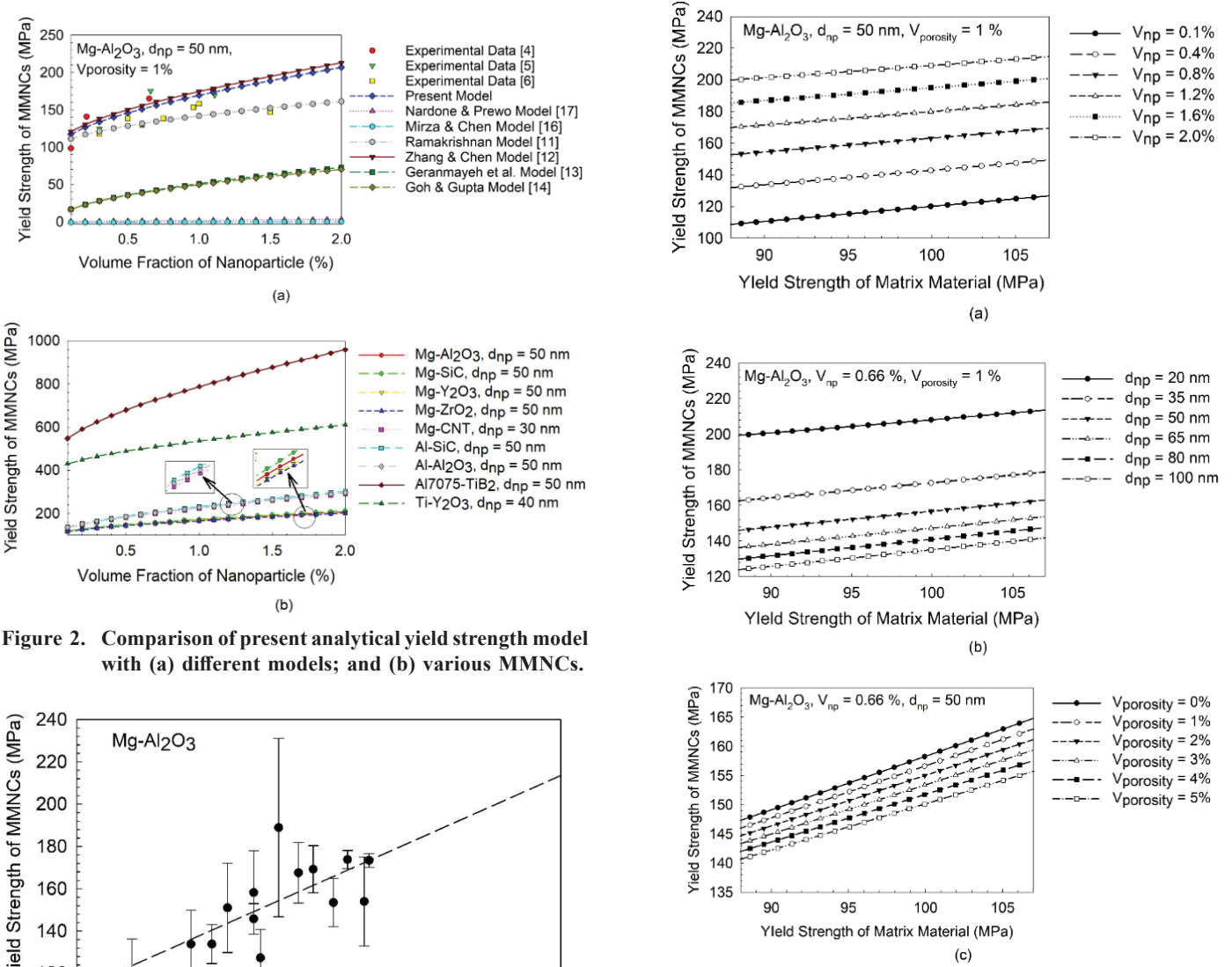


Figure 2. Comparison of present analytical yield strength model with (a) different models; and (b) various MMNCs.

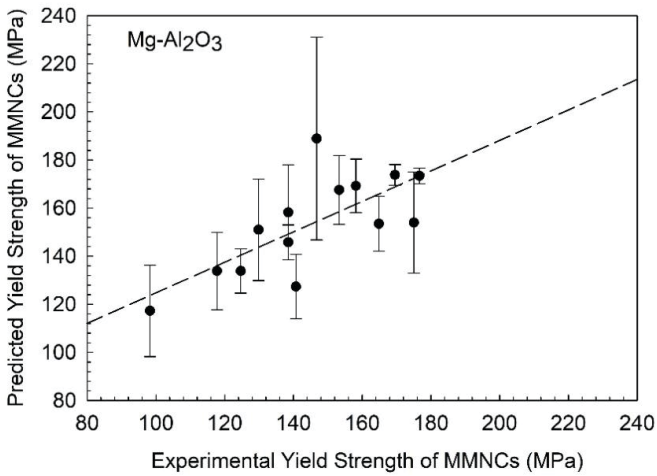


Figure 3. Comparison of the present analytical yield strength model with experimental data for Mg-Al₂O₃.

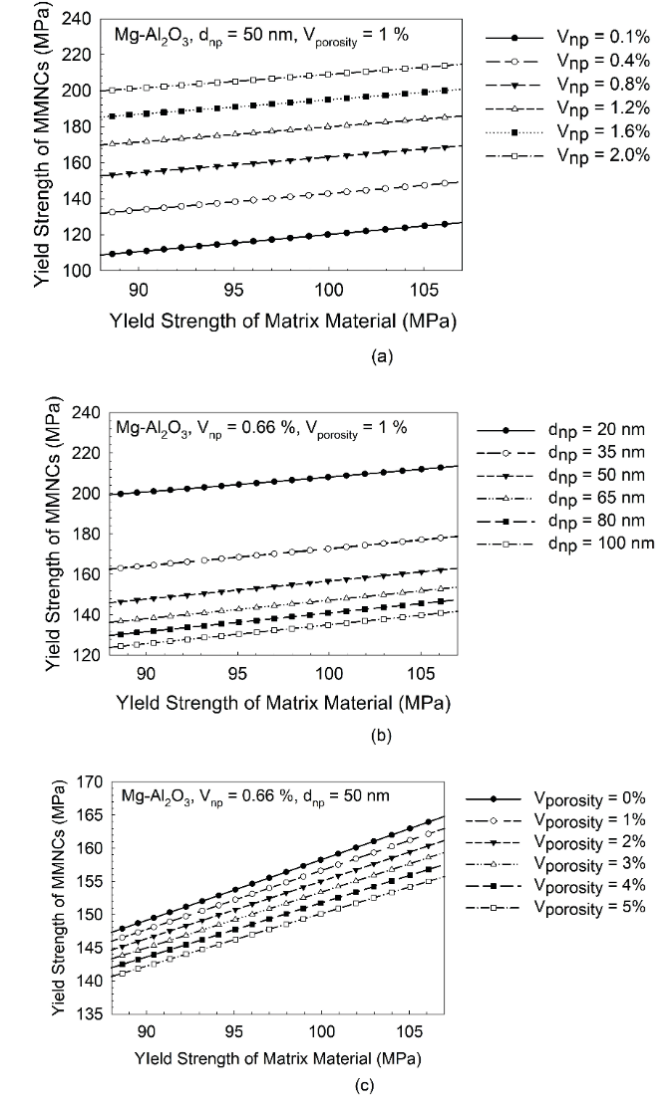


Figure 4. Comparison between the MMNCs and the matrix's yield strength: (a) volume fraction of nanoparticles (V_{np}), (b) nanoparticle diameter (d_{np}), (c) volume fraction of porosity in matrix material (V_p), as a parameter.

yield strength of different MMNCs increases with the volume fraction of nanoparticles.

The study focuses on the relationship between experimental measurements and model-based predictions for Mg-Al₂O₃ MMNC. The model predictions follow a linear trend

until the yield strength reaches 170 MPa, after which the trend is asymptotic, as shown in Fig. 2(b). However, after 170 MPa, the predicted yield strength values are underestimated. The study model can predict yield strength with near accuracy up to 170 MPa for Mg-Al₂O₃ MMNC. However, significant positive deviations between predicted yield strengths and experimental results remain uncertain. The model prediction for nano-sized reinforcing particles agrees with experimental data (Fig. 3), considering the variation in nanoparticle volume fraction, thermomechanical treatment, and microstructure. This helps to determine the active strain arising from residual thermal stresses.

5.2 Effect of Matrix Yield Strength

The study evaluates the impact of Mg matrix material (σ_{ym}) on Mg-Al₂O₃ MMNCs (σ_{ync}) with different V_{np} values (0.1 %, 0.4 %, 0.8 %, 1.2 %, 1.6 %, and 2.0 %) as depicted in Fig. 4(a). As the nanocomposite volume percentage increases, the yield strength of MMNCs increases by 69.29 % compared to the matrix yield strength. The larger volume fraction of the nanoparticle results in higher yield strength. Nanoparticles possess superior strength and stiffness compared to the matrix material, serving as effective reinforcements that enhance composite rigidity, resist deformation, and efficiently distribute and transmit applied loads^{5,10,42-43}.

The yield strength of Mg-Al₂O₃ MMNCs decreases as the size of nanoparticles (d_{np}) increases, with a reduction of 45.45 % relative to the matrix yield strength (Fig. 4(b)). The decrement is due to the heterogeneity in the matrix, which reduces their ability to resist dislocation, deformation, and stress concentration^{5,44}. Larger particles under tension result in localized stress concentrations, weakening the material^{5,10}

and potentially leading to premature failure⁴⁴. Additionally, increasing nanoparticle diameters reduces surface area for matrix bonding, resulting in weak contact bonding and reduced yield strength and load transfer efficiency. Pore stress concentrations also lower yield strength and stiffness in composite materials during manufacturing^{5,10,42,44}. For these reasons, the overall yield strength of MMNCs decreases as nanoparticle size increases^{42,44}.

As the porosity in the matrix material in the nanocomposite increases (Fig. 4(c)), the yield strength of MMNCs decreases overall by 5.50 % for the matrix yield strength, due to lower stress. These conclusions are in good agreement with the experimental observations⁶. Further, the higher yield strength of the matrix material results in higher yield strength of MMNCs at any given V_p , in good agreement with the literature for MMNCs^{6,28,43}.

5.3 Effect of the Orowan Strengthening Mechanism

Figure 5(a) demonstrates the impact of rigid nanoparticles on the yield strength of MMNCs, specifically Orowan strengthening (Eqn. 18). To accurately predict the strength, it’s crucial to consider both thermal mismatch and the Orowan mechanism⁶. The absence of Orowan strengthening in Al₂O₃ nanoparticle-reinforced Mg nanocomposite leads to underestimated strength predictions. Fig. 5(a) suggests that increasing the nanoparticle volume percentage can enhance the yield strength of MMNCs.

Figure 5(b) shows the effect of interparticle spacing of nanoparticles in the matrix material on the yield strength of MMNCs. The generalized equation of Orowan strengthening mechanism is given as:

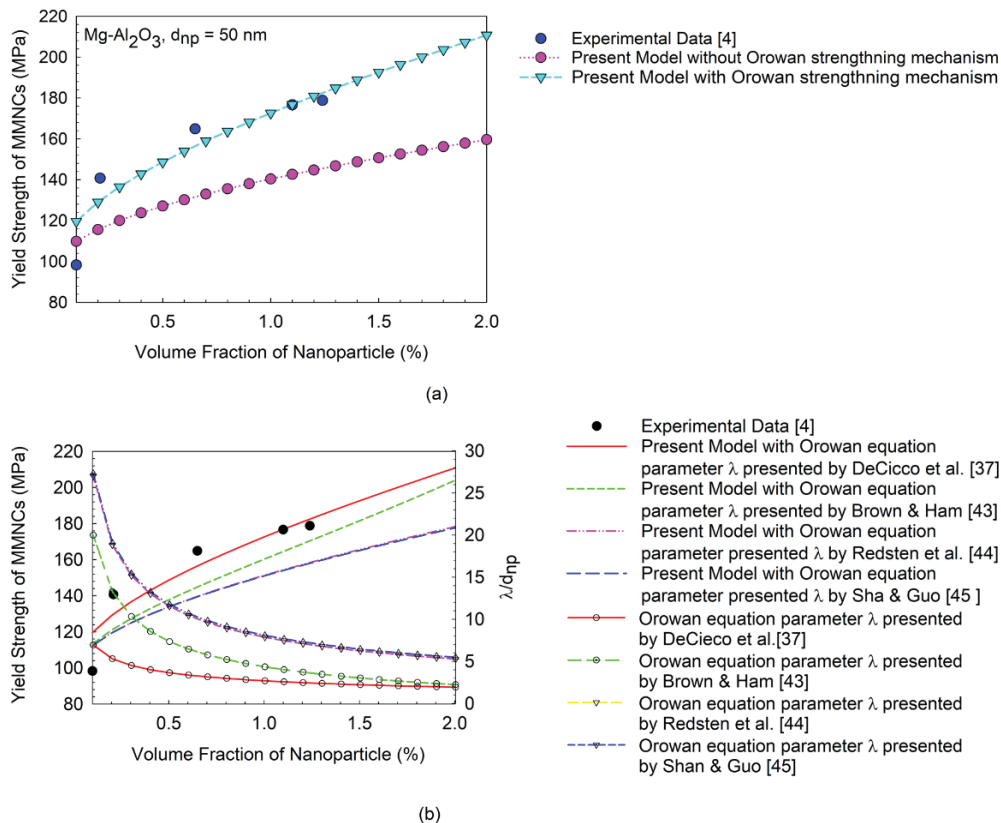


Figure 5. Effect of Orowan strengthening mechanism: (a) Present model v/s experimental data; and (b) Interparticle spacing.

Table 2. Orowan equation parameters utilized by different researchers

Method	C	λ/d_{np}	X
DeCicco ³⁹ , <i>et al.</i>	$\frac{1}{8}$	$\left(\frac{1}{2V_{np}}\right)^{\frac{1}{3}} - 1$	2
Brown & Ham ⁴⁵	$\frac{0.8}{2\pi\sqrt{1-\nu}} \cong \frac{1}{6}$	$\frac{1}{2} \left[\left(\frac{2\pi}{3V_{np}}\right)^{\frac{1}{3}} - 2\left(\frac{2\pi}{3}\right)^{\frac{1}{2}} \right]$	2
Redsten ⁴⁶ , <i>et al.</i>	$\frac{0.4M}{\pi\sqrt{1-\nu}} \cong \frac{1}{2}$	$\left(\frac{1}{4V_{np}}\right)^{\frac{1}{2}} - 1$	$\sqrt{\frac{3}{2}}$
Sha & Guo ⁴⁷	$\frac{0.8(1.2)}{2\pi} \cong \frac{1}{6}$	$\frac{1.23}{2} \left[\left(\frac{2\pi}{3V_{np}}\right)^{\frac{1}{2}} - \sqrt{\frac{2}{3}} \right]$	2

$$\Delta \sigma_{Orowan} = C \frac{G_m b}{\lambda} \ln \left(\frac{d_{np}}{Xb} \right) \quad (24)$$

In the above Eqn. (24) the inter-particles spacing λ and matrix dislocation parameter $\ln \left(\frac{d_{np}}{Xb} \right)$ are important parameters in the Orowan strengthening mechanism. Various Orowan strengthening mechanism models are available in literature^{39,45-47} and presented in Table 2. The equations pertaining to $\frac{\lambda}{d_{np}}$, as presented in Table 2, are derived from the assumption of a symmetrical array of evenly spaced particles. Table 2 describes the interparticle mean free path for dislocation motion, calculated by subtracting the average distance between particle centers from the average particle diameter. The DeCicco³⁹, *et al.* model is the best fit with experimental data for Mg-Al₂O₃. The distance dislocations can bow out influences the mean free path distance in impermeable particles^{5,16,17}, which can be calculated by subtracting the average dispersoid diameter from the average dispersoid spacing distance¹⁶.

5.4 Effect of Porosity

The yield strength (σ_{ync}) of Mg-Al₂O₃ MMNCs is predicted for varying (V_{np}) values, indicating that more porosity leads to lower yield strength due to reduced stress (Fig. 6(a)). This is consistent with experimental observations⁶. Increasing nanoparticle volume fraction leads to a larger yield strength at any given (V_{np}), which is consistent with literature findings for MMNCs^{6,28,43}. An increase in the volume fraction of Al₂O₃ nanoparticles reinforced in the Mg matrix leads to a corresponding rise in yield strength⁶. Conversely, as the size of nanoparticles (d_{np}) in Mg-Al₂O₃ MMNCs increases, the yield strength decreases, as seen in Fig. 6(b). For all sizes of reinforcement (d_{np}), increased porosity leads to decreased yield strength. The combined impact of the V_{np} and d_{np} plot (Fig. 6(c)) illustrates the regions where the volume fraction and nanoparticle size substantially influence the yield strength. In general, an increase in the volume fraction of nanoparticles leads to an increase in yield strength, while an increase in the diameter of nanoparticles reduces yield strength.

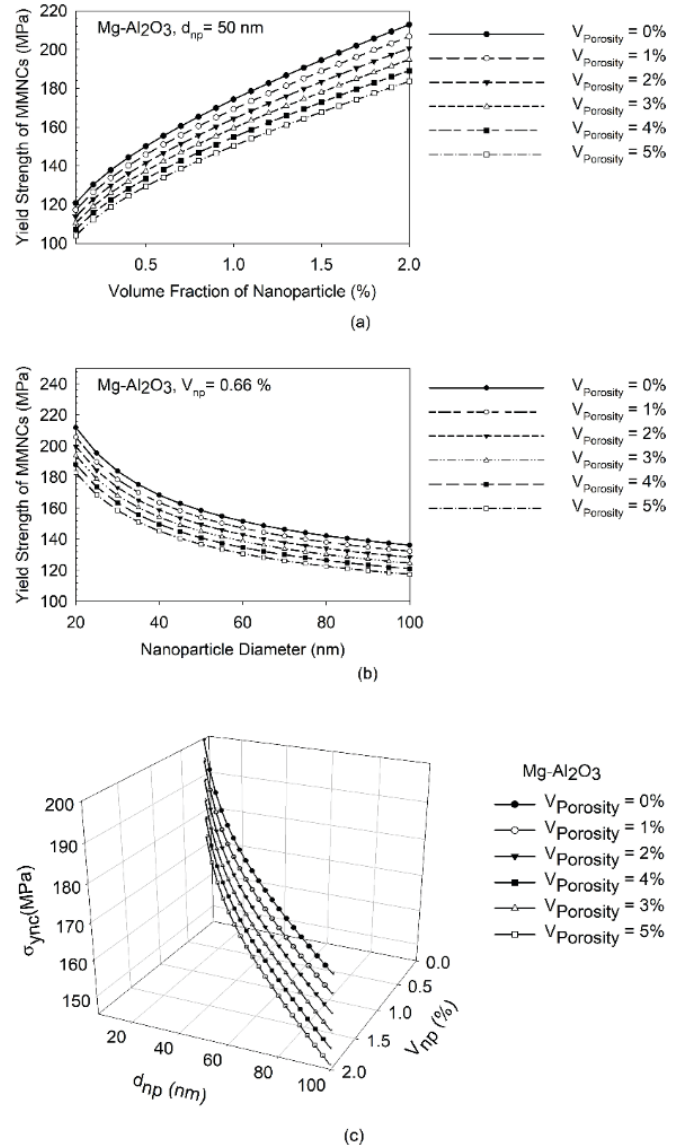


Figure 6. Effect of porosity (V_{np}) on yield strength (σ_{ync}) of Mg-Al₂O₃ MMNCs: (a) volume fraction of nanoparticles (V_{np}), (b) nanoparticle diameter (d_{np}), (c) combined effect of V_{np} and d_{np} .

5.5 Agglomerated State of Nanoparticles into the Metal Matrix

Agglomeration in a metal matrix is crucial for creating nanocomposites, as it directly deviates/alters their properties and performance. During the processing, nanoparticles aggregate and form clusters and agglomerates inside the matrix because of interparticle forces and surface interactions. Figure 7 depicts the influence of agglomeration in the Mg-Al₂O₃ MMNCs, while maintaining a constant volume fraction and diameter of the nanoparticles. The variable ξ_b represents the proportion of agglomeration inside the matrix, with a higher value indicating more pronounced nanoparticle aggregation. When ξ_b equals 1, all nanoparticles are uniformly dispersed, causing a decline in structural integrity.

When ξ_b equals λ_b , all nanoparticles are uniformly dispersed throughout the MMNCs and the value of $\sigma_{agg,nc}$ is 153.98 MPa. For agglomeration to occur in MMNCs, ξ_b must be larger than λ_b , resulting in a more diverse and uneven spatial distribution of nanoparticles. Agglomerates create imperfections and areas of concentrated stress, promoting fracture propagation and reducing the overall durability of MMNCs³⁶⁻³⁷. This reduces yield strength and makes the material more susceptible to deformation under stress^{30,34-35,48}. A higher concentration of nanoparticles inside agglomerates leads to a decrease in the overall strength and stiffness of the MMNCs^{29-30,32,34,35,48}.

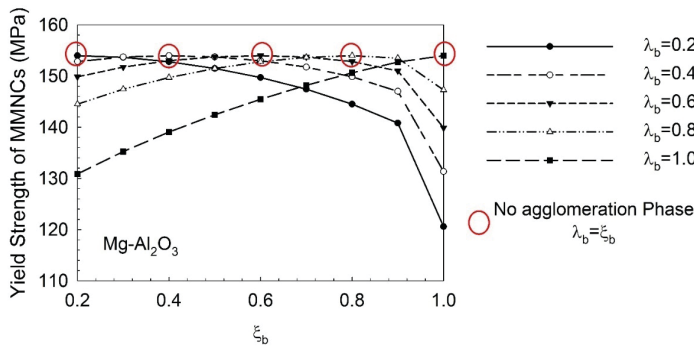


Figure 7. Effect of agglomeration in MMNCs.

5.5.1 Complete Agglomeration of Nanoparticles in the Matrix ($\lambda_b = 1$)

The influence of agglomeration on the yield strength of Mg-Al₂O₃ MMNCs by examining the effects of volume fraction (V_{np}) and diameter (d_{np}) of nanoparticles. The condition λ_b is equal to 1 indicates that the nanoparticles have fully agglomerated, resulting in a spherical area classified as an inclusion (Fig. 2). If the assumption regarding spherical agglomeration is invalid, the actual material performance could vary from the predictions of the current model due to ineffective load transfer, weak interfaces, and modified strengthening mechanisms⁵.

Figure 8(a) demonstrates that the volume fraction of agglomeration decreases as the volume fraction of nanoparticles increases, indicating an inverse connection between ξ_b and yield strength. Larger aggregates indicate reduced strength compared to individual and scattered nanoparticles. Interactions between particles, such as Van der Waals forces, may cause particles to aggregate together and restrict stress transmission, leading

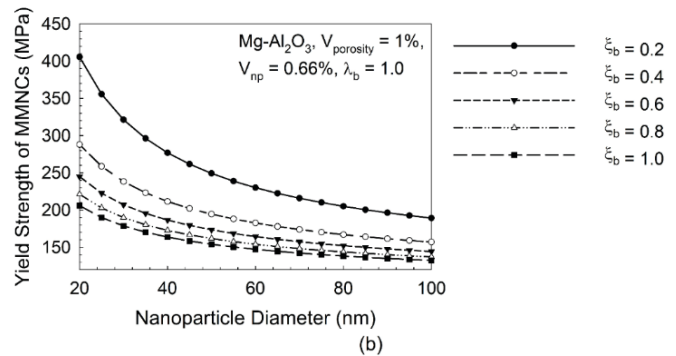
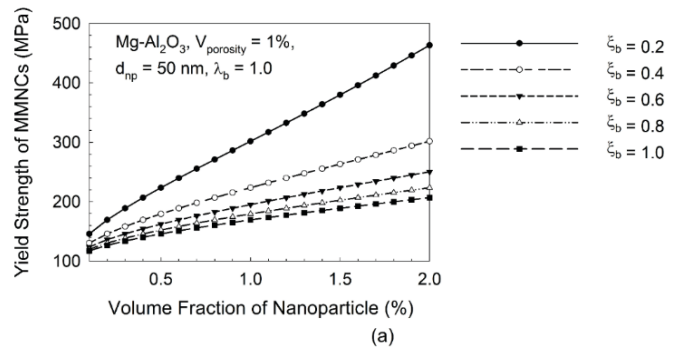


Figure 8. Effect of nanoparticle complete agglomeration ($\lambda_b = 1$) on yield strength (σ_{nc}), MPa of Mg-Al₂O₃ MMNCs: (a) volume fraction of nanoparticles (V_{np}), (b) nanoparticle diameter (d_{np}) as a parameter.

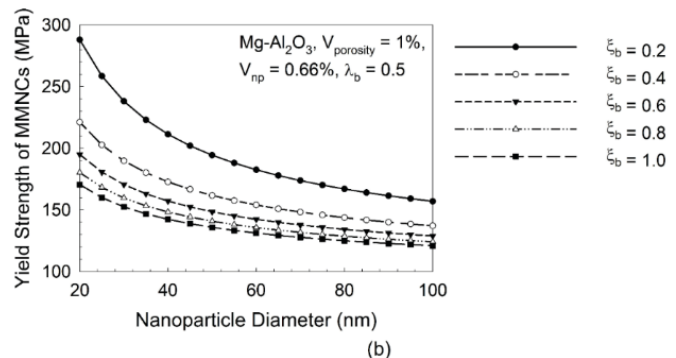
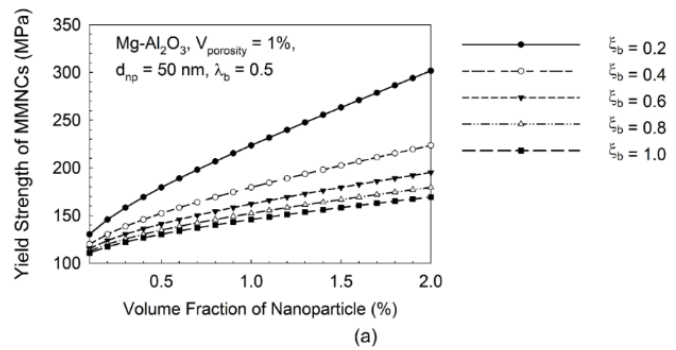


Figure 9. Effect of nanoparticle complete agglomeration ($\lambda_b = 0.5$) on yield strength (σ_{nc}), MPa of Mg-Al₂O₃ MMNCs: (a) volume fraction of nanoparticles (V_{np}), (b) nanoparticle diameter (d_{np}) as a parameter.

to a decrease in yield strength^{30,48}. The presence of voids and gaps in the agglomerated structure may also decrease density, elastic modulus, and strength³⁶⁻³⁷. Stress may lead to localized deformation or failure, resulting in a decrease in overall yield

strength. To achieve the required properties, it is crucial to ensure uniform dispersion of nanoparticles. Figure 8(b) illustrates the impact of nanoparticle agglomeration on the yield strength of Mg-Al₂O₃ MMNCs, with the nanoparticle diameter as a parameter. For a certain nanoparticle diameter (d_{np}), the ξ_b value is inversely proportional to the yield strength. This indicates that increased agglomeration leads to a decrease in yield strength. Nanoparticles with reduced diameters demonstrate increased surface area-to-volume ratios and surface energy⁴⁸⁻⁴⁹.

5.5.2 Partial Agglomeration of Nanoparticles in the Matrix ($\lambda_b=0.5$)

The impacts of volume fraction (V_{np}) and diameter (d_{np}) of nanoparticles under partial agglomeration of nanoparticles in the matrix ($\lambda_b=0.5$) are being examined to explore the influence of agglomeration on the yield strength of Mg-Al₂O₃ MMNC. Figure 9(a) demonstrates the effect of partial agglomeration ($\lambda_b=0.5$) of nanoparticles on the yield strength of Mg-Al₂O₃ MMNCs, with the volume fraction as the variable. Figure 9(b) demonstrates the influence of partial agglomeration on the yield strength of Mg-Al₂O₃ MMNCs, where the variable is the diameter of the nanoparticles. Partial agglomeration may have lesser effect on mechanical characteristics in comparison to complete agglomeration, but it may still result in deviations from the specified performance parameters⁴⁸⁻⁴⁹.

Both the cases discussed in sections 5.5.1 and 5.5.2 investigate the impact of the volume fraction (V_{np}) and diameter (d_{np}) of nanoparticles on the yield strength during the agglomeration state. These variables impact the degree of agglomeration and, as a result, the mechanical characteristics of the composite material. Higher nanoparticle concentration and reduced nanoparticle sizes lead to a reduction in aggregation and enhance the yield strength of MMNC. The degree of agglomeration, nanoparticle-matrix interactions, and processing conditions influence the correlation between these components and the yield strength^{29,35,48}.

5.6 Sensitivity Analysis

The present study establishes a relationship between eleven input microstructural modeling parameters such as (i) V_{np} , (ii) λ_b , (iii) ξ_b , (iv) d_{np} , (v) $\Delta\alpha$, (vi) ΔT , (vii) b , (viii) k , (ix) G_m , (x) V_p and (xi) ϕ and the output yield strength of Mg-Al₂O₃ MMNC. The deviation is calculated for each input parameter within the variability of $\pm 10\%$ of the mean value (Table 1). The effect of each microstructural parameter on the yield strength is analyzed (Fig. 10) by fixing the other parameters at their mean values, which depicts that V_{np} reduces the yield strength by 3.08 % or increases by 3.26 %, λ_b reduces by 2.15 % or increases by 2.02 % and ξ_b reduces by 2.15 % or increases by 2.02 %, d_{np} reduces by 2.83 % or increases by 2.38 %, $\Delta\alpha$ reduces by 1.25 % or increases by 1.31 %, ΔT reduces by 1.37 % or increases by 1.32 %, b reduces by 0.17 % or increases by 0.05 %, k reduces by 2.82 % or increases by 2.57 %, G_m reduces by 4.58 % or increases by 4.07 %, V_p reduces by 0.28 % or increases by 0.31 % and ϕ reduces by 0.19 % or increases by 0.20 %. It is concluded that V_{np} , λ_b , ξ_b , d_{np} , k , and G_m are more sensitive parameters than the $\Delta\alpha$, ΔT , b , k , V_p and ϕ for

the estimation of the yield strength.

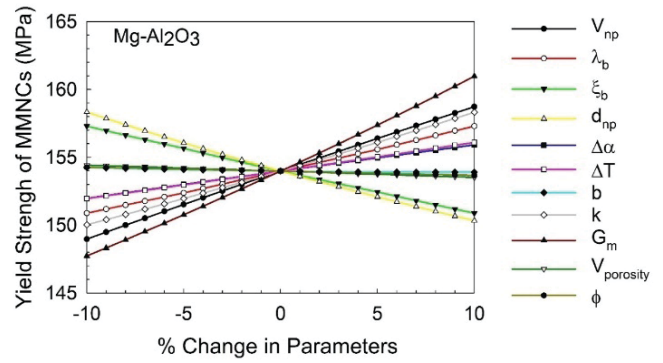


Figure 10. The sensitivity analysis using the various modeling parameters (V_{np} , λ_b , ξ_b , d_{np} , $\Delta\alpha$, ΔT , b , k , G_m , V_p and ϕ) on the yield strength of Mg-Al₂O₃ MMNCs.

6. CONCLUSIONS

This study investigates the mechanical properties of MMNCs, focusing on porosity and nanoparticle agglomeration. It develops and evaluates a predictive model for the yield strength of MMNCs, comparing it with other models and experimental data. The model predicts MMNC behaviour in Al₂O₃ nanoparticle-reinforced Mg matrices, including several strengthening factors incorporating Orowan strengthening. The analysis shows that an increase in nanoparticle volume fraction from 0.1 % to 2.0 % leads to an enhancement of 69.29 % yield strength, while higher nanoparticle sizes (from 20 to 100 nm) and greater porosity levels (from 0 % to 5 %) result in a 45.45 % and 5.50 % reduction in yield strength, respectively. Further, the study highlights the adverse effect of nanoparticle agglomeration on MMNC mechanical characteristics, causing regional stress and structural defects and highlights the need for nanoparticle uniformity in composites manufacturing. The model reliability is analysed, providing insights for future optimization efforts. The study concludes that the yield strength predictive model may improve understanding of MMNCs mechanical properties and enhance reliability in designing composites for exceptional structural performance.

REFERENCES

1. Ramnath, BV, Elanchezian C, Annamalai, RM, et al. Aluminium metal matrix composites—a review. *Rev Adv Mater Sci* 2014;38(5):55–60.
2. Ibrahim, IA, Mohamed, FA, Lavernia, EJ. Particulate reinforced metal matrix composites—a review. *J Mater Sci* 1991;26(5):1137–1156.
3. Rohatgi, PK. Metal matrix Composites. *Def Sci J* 1993;43(4):323–349.
4. Bansal S, Saini JS. Mechanical and Wear Properties of SiC/Graphite Reinforced Al359 Alloy-based Metal Matrix Composite. *Def Sci J* 2015;65(4):330.
5. Ceschini, L, Dahle, A, Gupta, M, et al. Aluminum and magnesium metal matrix nanocomposites. Springer, 2017.
6. Hassan, SF, Gupta, M. Development of high performance magnesium nanocomposites using solidification processing route. *Materials Science and Technology*

- 2004;20(11):1383–1388.
7. Hassan, SF, Tan, MJ, Gupta, M. High-temperature tensile properties of Mg/Al₂O₃ nanocomposite. *Materials Science and Engineering: A* 2008;486(1–2):56–62.
 8. Zhong, XL, Wong, WLE, Gupta, M. Enhancing strength and ductility of magnesium by integrating it with aluminum nanoparticles. *Acta Mater* 2007;55(18):6338–6344.
 9. Kurahatti, R, Surendranathan A, Kori S, Singh N, Kumar A, Srivastava S. Defence applications of polymer nanocomposites. *Def Sci J* 2010;60(5):551–563.
 10. Ferguson, JB, Lopez, HF, Rohatgi, PK, Cho, K, Kim, C-S. Impact of volume fraction and size of reinforcement particles on the grain size in metal–matrix micro and nanocomposites. *Metallurgical and Materials Transactions A* 2014;45(9):4055–4061.
 11. Chawla D, Nayak, M, Gupta, P. Investigating the effect of particle sizes of SiC and graphite on strengthening of aluminium metal matrix composites. *ECS Journal of Solid State Science and Technology* 2024;13(2): 021002.
 12. Gupta, S, Tevatia, A, Rana, KPS. A fatigue crack growth life prediction model for metal matrix nanocomposites: contribution of strengthening factors. *Advanced Composite Materials* 2022;31(1):43–61.
 13. Tevatia, A, Srivastava, SK. The energy-based multistage fatigue crack growth life prediction model for DRMMC s. *Fatigue Fract Eng Mater Struct* 2018;41(12):2530–2540.
 14. Taya M, Arsenault, RJ. A comparison between a shear lag type model and an eshelby type model in predicting the mechanical properties of a short fiber composite. *Scripta Metallurgica* 1987;21(3):349–354.
 15. Jiang ZH, Lian, JS, Dong SL, Yang DZ. An application of the modified shear lag model to study the influence of thermal residual stresses on the strength and yield strength of short fiber reinforced metal matrix composites. *J Mater Sci Technol* 1999;15(3):213–221.
 16. Zhang Z., Chen, DL. Consideration of Orowan strengthening effect in particulate-reinforced metal matrix nanocomposites: A model for predicting their yield strength. *Scr Mater* 2006;54(7):1321–1326.
 17. Zhang Z, Chen, DL. Contribution of Orowan strengthening effect in particulate-reinforced metal matrix nanocomposites. *Materials Science and Engineering: A* 2008;483:148–152.
 18. Scattergood, RO, Bacon, DJ. The Orowan mechanism in anisotropic crystals. *Philosophical Magazine* 1975;31(1):179–198.
 19. Ramakrishnan, N. An analytical study on strengthening of particulate reinforced metal matrix composites. *Acta Mater* 1996;44(1):69–77.
 20. Geranmayeh, AR, Mahmudi, R, Kangoorie, M. High-temperature shear strength of lead-free Sn-Sb-Ag/Al₂O₃ composite solder. *Materials Science and Engineering: A* 2011;528(12):3967–3972.
 21. Goh, CS, Gupta, M, Wei, J, Lee, LC. Characterization of high performance Mg/MgO nanocomposites. *J Compos Mater* 2007;41(19):2325–2335.
 22. Mirza FA, Chen DL. An analytical model for predicting the yield strength of particulate-reinforced metal matrix nanocomposites with consideration of porosity. *Nanoscience and Nanotechnology Letters* 2012;4(8):794–800.
 23. Nardone VC, Prewo KM. On the strength of discontinuous silicon carbide reinforced aluminum composites. *Scripta Metallurgica* 1986;20(1):43–48.
 24. Ahmad, SN, Hashim, J, Ghazali, MI. The effects of porosity on mechanical properties of cast discontinuous reinforced metal- matrix composite. *J Compos Mater* 2005;39(5):451–466.
 25. Ahmad,SNAS, Hashim, J, Ghazali, MI. Effect of porosity on tensile properties of cast particle reinforced MMC. *J Compos Mater* 2007;41(5):575–589.
 26. William Brassell, G, Horak, JA, Ridge, O, Lynn Butler, B. Effects of porosity on strength of carbon-carbon composites. 2015;
 27. Molina, JM, Prieto, R, Narciso, J, Louis, E. The effect of porosity on the thermal conductivity of Al-12 wt.% Si/SiC composites. *Scr Mater* 2009;60(7):582–585.
 28. Sahoo, BP, Das, D, Chaubey, AK. Strengthening mechanisms and modelling of mechanical properties of submicron-TiB₂ particulate reinforced Al 7075 metal matrix composites. *Materials Science and Engineering: A* 2021;825.
 29. Pan, J, Bian, L. Influence of agglomeration parameters on carbon nanotube composites. *Acta Mech* 2017;228(6):2207–2217.
 30. Golbang, A, Famili, MHN, Shirvan, MMM. A method for quantitative characterization of agglomeration degree in nanocomposites. *Compos Sci Technol* 2017;145:181–186.
 31. Pan, J, Bian, L. A physics investigation for influence of carbon nanotube agglomeration on thermal properties of composites. *Mater Chem Phys* 2019;236.
 32. Qiao, R, Deng, H, Putz, KW, Brinson, LC. Effect of particle agglomeration and interphase on the glass transition temperature of polymer nanocomposites. *J Polym Sci B Polym Phys* 2011;49(10):740–748.
 33. Zare, Y. Modeling the yield strength of polymer nanocomposites based upon nanoparticle agglomeration and polymer-filler interphase. *J Colloid Interface Sci* 2016;467:165–169.
 34. Shi, DL, Feng, XQ, Huang, YY, Hwang, KC, Gao, H. The effect of nanotube waviness and agglomeration on the elastic property of carbon nanotube-reinforced composites. *J Eng Mater Technol* 2004;126(3):250–257.
 35. Karevan, M, Pucha, RV., Bhuiyan, MdA, Kalaitzidou, K. Effect of interphase modulus and nanofiller agglomeration on the tensile modulus of graphite nanoplatelets and carbon nanotube reinforced polypropylene nanocomposites. *Carbon letters* 2010;11(4):325–331.
 36. Fadavi Boostani A, Taherzadeh Mousavian R, Tahamtan S, et al. Solvothermal-assisted graphene encapsulation of SiC nanoparticles: A new horizon toward toughening aluminium matrix nanocomposites. *Materials Science and Engineering: A* 2016;653:99–107.
 37. Liu W, Bian L. Influences of inclusions and corresponding

- interphase on elastic properties of composites. *Archive of Applied Mechanics* 2018;88(9):1507–1524.
38. Dunand DC, Mortensen A. On plastic relaxation of thermal stresses in reinforced metals. *Acta metallurgica et materialia* 1991;39(ARTICLE):127.
 39. Cicco M De, Konishi H, Cao G, et al. Strong, Ductile Magnesium-Zinc Nanocomposites. *Metallurgical and Materials Transactions A* 2009;40(12):3038–3045.
 40. Srivastava S, Tevatia A. Crack growth energetics to predict fatigue failures in particle-reinforced metal matrix composites (PRMMC). *Int J Fatigue* 2022;162:106985.
 41. Mirza FA, Chen DL. A unified model for the prediction of yield strength in particulate-reinforced metal matrix nanocomposites. *Materials* 2015;8(8):5138–5153.
 42. Malaki M, Xu W, Kasar AK, et al. Advanced metal matrix nanocomposites. *Metals (Basel)* 2019;9(3):330.
 43. Hassanzadeh-Aghdam MK, Mahmoodi MJ, Ansari R. A comprehensive predicting model for thermomechanical properties of particulate metal matrix nanocomposites. *J Alloys Compd* 2018;739:164–177.
 44. Soleymani Shishvan S, Asghari A-H. Effects of particle shape and size distribution on particle size-dependent flow strengthening in metal matrix composites. *scientiairanica* 2017;24(3):1091–1099.
 45. Brown LM, Ham RK. Dislocation-particle Interactions. In: Kelly A., Nicholson RB, editors. *In Strengthening Methods in Crystals*. Amsterdam, The Netherlands: Elsevier, 1971;
 46. Redsten AM, Klier EM, Brown AM, Dunand DC. Mechanical properties and microstructure of cast oxide-dispersion-strengthened aluminum. *Materials Science and Engineering: A* 1995;201(1–2):88–102.
 47. Sha W, Guo Z. *Maraging steels: Modelling of microstructure, properties and applications*. Woodhead Publishing., 2009;
 48. Pouyanmehr R, Hassanzadeh-Aghdam MK, Ansari R. Estimation of elastic modulus and Poisson's ratio of concrete containing graphene nanosheets: A focus on nano-filler agglomeration and hydration time. *Computational Sciences and Engineering* 2022;2(1):111–123.
 49. Chen S, Hassanzadeh-Aghdam MK, Ansari R. An analytical model for elastic modulus calculation of SiC whisker-reinforced hybrid metal matrix nanocomposite containing SiC nanoparticles. *J Alloys Compd* 2018;767:632–641.

CONTRIBUTORS

Mr Sanjay Gupta is an Associate Professor at NSUT. His research interests include: Computational modeling techniques, fatigue analysis, and metal matrix nanocomposites. In the current study, he formulated the research problem, contributed to interpreting the results, and drafted sections of the manuscript.

Dr Abhishek Tevatia is an Assistant Professor at NSUT. His research interests include: Computational modeling techniques, finite element fatigue analysis, and design sensitivity and uncertainty analysis. In the current study, his major role was in finalizing the work plan, correlating the results, and reviewing the manuscript to ensure clarity, accuracy, and coherence.

Prof (Dr) KPS Rana is working at NSUT. His research interests include: Measuring circuits and instrumentation, system modeling and renewable energy. In the current study he offered guidance and support for the current study and reviewed the manuscript.